Indian Journal of Pure & Applied Physics
Vol. 53, October 2015, pp. 691-695

Investigation of Cu_2ZnSnS_4 thin film by scanning Kelvin force microscopy

Om Pal Singh[1,2], Nadarajah Muhunthan[1,2] & Vidya N Singh[1,2*]

[1]Academy of Scientific and Innovative Research (AcSIR),

[2]CSIR-National Physical Laboratory, Dr. K. S. Krishnan Marg, New Delhi 110 012, India

*E-mail:singhvn@nplindia.org

Received 13 November 2014; revised 2 June 2015; accepted 12 August 2015

CZTS thin film has been grown on Mo-coated soda lime glass by co-sputtering the metal targets and post sulfurization in H_2S ambient. The structural, microstructural, compositional and optical properties have been studied using glancing incidence XRD, Raman spectroscopy, SEM, EDS, XRF and UV-Vis spectrophotometry. Local electrical transport measurements using conducting AFM show that for small bias voltage (–0.5 V), the dark negative currents flow mainly through grain boundaries (GBs) rather than grain interior. Kelvin probe force microscopic measurements (local surface potential) indicated positive surface potential in the vicinity of GBs in a Cu-deficient CZTS thin film. All measurements indicated that grain interior to GBs have a smaller effective band gap than the bulk, due to the composition change (Cu-vacancies or Cu_{Zn} anti site defects) at GBs. Electrical measurement revealed the presence of defects in the CZTS thin film.

Keywords: CZTS, Sputtering, Sulfurization using H_2S, C-AFM, Structural properties

1 Introduction

Polycrystalline thin film solar cells based on Cu $(In,Ga)(Se,S)_2$ (CIGS) and CdTe have improved significantly over recent years[1]. However, both materials are constrained by rareness and environmental hazard issues. An alternative compound, Cu_2ZnSnS_4 (CZTS) is regarded as a new promising material for polycrystalline thin film solar cells. A band gap of 1.4 ~ 1.5 eV and absorption coefficient above 10^4 cm^{-1} in visible spectrum range[2,4] makes CZTS an optimal material for thin film solar cell. The band gap of the compound $Cu_2ZnSnSe_4$ and $Cu_2ZnSn(S_{1-x},Se_x)_4$ can be tuned[5,6] by using Se. Both Zn and Sn are non-toxic and their abundance in the earth-crust is 75 and 2.2 ppm, respectively while that of indium is only 0.049 ppm. For the deposition of CZTS thin film, several techniques such as sputtering[7], spray pyrolysis[8], electrodeposition[9], co-evaporation[10], pulsed laser deposition[11] and nano particle route[12] have been used. Considering the high material utilization ratio and availability of existing sophisticated facilities, sputter deposition has the potential to be scaled up for large-area production. Typically, CZTS layers are produced by sulfurization of as-deposited metallic films or stacked metal sulfide films. The highest reported efficiency of CZTS solar cells by co-sputtering of ZnS, SnS and Cu targets with *RF* power followed by sulfurizing in the atmosphere of hydrogen sulfide is 6.7%[13]. The record efficiency for selenium doped $Cu_2ZnSn(S,Se)_4$ is 12.6%[14]. Several losses in a solar cell are summarized[15]. In the present study, we have deposited Cu-poor co-sputtered CuZnSn (CZT) layers, and sulfurized the layers to convert it into CZTS. The fabricated CZTS films are characterized by X-ray diffraction (XRD), scanning electron microscopy (SEM), energy dispersive spectroscopy (EDS) and Raman scattering measurements. Work based on synthesis and characterization of CZTS thin films by our group has already been reported[16,17].

The conduction behavior of CZTS is a key characteristic. The absorption layer must have a long carrier life time and diffusion length. The grain boundaries (GB) of polycrystalline CZTS thin films are believed to have a built-in potential, which play an important role in the device conversion efficiency[9,10]. Polycrystalline CZTS thin films exhibit better solar cell efficiency than single crystalline[7,11]. Therefore, the structural and electrical properties related to the grain boundaries are important issues to consider while attempting improving the solar cell performance[10-14].

2 Experimental Details

2.1 Materials

All the three targets Cu, Zn and Sn (obtained from Vin Karola USA, 2 inch diameter, 3 mm thickness) were 99.99% or more pure. H_2S gas (diluted with 85 vol % Ar) with 99.99% purity and Ar (99.9999%

pure) were purchased from BOC India limited. N_2 gas (99.9% pure), reagent grade acetone and propanol were supplied by the local suppliers in India.

2.2 Synthesis and Characterization

In the present study, CZTS thin films were synthesized using co-sputtering and sulfurizing it in H_2S at 550°C. Cu, Zn and Sn targets were used as source material. Cu was sputtered using 12 W *dc* power and Zn and Sn were sputtered using 75 W and 55 W *RF* power. Substrate rotation was set to 5 rpm during deposition. The film was deposited at ambient temperature on soda lime glass (SLG) substrate. Prior to deposition, SLG substrates were cleaned in acetone, propanol and deionized water. The chamber pressure before deposition and during the deposition was maintained at 1.0×10^{-6} mbar and 5.0×10^{-3} mbar, respectively. During the growth of CZT layer, Ar gas flow rate was maintained at 30 sccm. The experiments were carried out to optimize the rate and power for the CZTS deposition[18]. The rapid sulfurization is performed in a horizontal tube furnace. In the furnace, mixed H_2S (15%)/Ar (85%) is flown continuously with a flow rate of 30 sccm for 30 min and the sulfurization temperature was maintained at 550°C. The sputtering time was adjusted to obtain 1.3 μm thick CZTS film. Optical properties were studied using UV-VIS spectrophotometer (Model: Shimadzu UV-VIS 1800). Structural properties were studied using GAXRD and Raman spectroscopy (Philips X'pert pro X-ray diffractometer). GAXRD is used to analyse the phase of material. Surface morphology (SEM model: Zeiss EVO-50, scanning electron microscope) and elemental composition were studied using scanning electron microscopy and energy dispersive spectrometry (EDS), respectively.

Multimode AFM with Nanoscope V controller, (Veeco Ltd, USA) is used for all AFM studies. For current mapping, an extended Tunneling Atomic Force Microscopy (TUNA) module, Bruker AXS was used along with Pt coated AFM tips. For conductivity mapping, the current sensitivity of the amplifier was set to 100 nA/V and scanned at 0.2 V sample bias. For Kelvin probe force microscopy, Pt coated tip biased at *ac*-amplitude of 1 V and a frequency of 80 kHz was used in interleave scan. Potential mode with a lift height of 50 nm was used.

3 Results and Discussion

3.1 Optical Properties

Optical spectrophotometer has been used for studying the optical properties of CZTS. From optical spectrophotometer results, band gap of material can be determined using the Tauc's plot; $(\alpha h\nu)^2$ versus $h\nu$ (shown in the inset of Fig. 1(a)). Using the long wavelength extrapolation of the band edge, a band gap value of 1.46 eV is estimated. The observed band gap value of 1.46 eV is optimal for solar cell applications. This observation also eliminates co-existence of secondary phase of ZnS (3.68 eV) and Cu_2SnS_3 (0.93eV) [19].

EDS result of the precursor indicates that the layer is Cu-poor ([Cu]/([Zn]+[Sn]) = 0.85) and slightly Zn-rich ([Zn]/[Sn] = 1.10). It is reported that Cu-poor Zn-rich precursors are good for enhanced efficiency of CZTS. Fig. 1 (b) shows SEM images at different magnifications of CZTS thin films fabricated by co-sputtering/sulfurization on soda lime glass. The film has good adherence to the substrate and is about 1.2 μm in thickness.

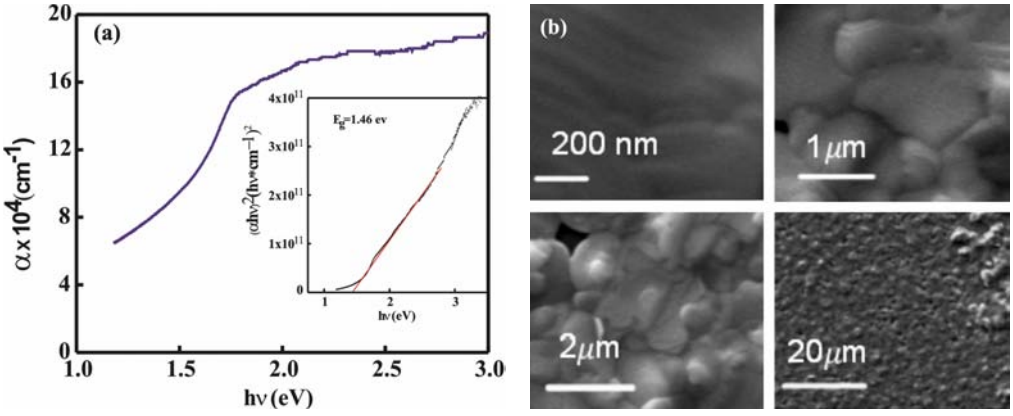

Fig. 1 — (a) Photon energy ($h\nu$) versus absorbance spectra, Tauc's plot is shown in the inset and (b) SEM micrographs at different magnification of same sample

Although few grains are observed on the surface of thin film, the micrograph shows closely packed grains and almost smooth surface. For better efficiency of polycrystalline thin film absorbers based solar cell, it is a necessary requirement to maximize both minority carrier diffusion length and built-in bias.

3.2 Structural properties

GAXRD pattern of the CZTS thin film is shown in Fig. 2(a) which indicates (112) oriented crystalline structure. It is known that when annealing is carried out at lower temperature, binary and ternary impurity phases appear[20-22]. In the GIXRD analysis, no peaks corresponding to $Cu_{2-x}S$ or any other phases are found.

Figure 2 (b) shows Raman scattering spectroscopy result of the CZTS film on SLG substrate. Raman peaks at ~165, ~288, ~338 and ~373 cm^{-1} are related to kesterite CZTS. A weak peak from $Cu_{2-x}S$ phase near 264 cm^{-1} is found in Raman spectroscopy.

3.3 Conducting AFM Studies (CAFM)

Earlier C-AFM study has been done on CIGS[23,24], CdTe and CZTS/CZTSe solar cells which have revealed higher current flow in the GBs of these materials[25,26]. This work also reveals a similar phenomenon occurring in CZTS thin films deposited by co-sputtering from metal targets and sulfurization using H_2S gas. Here, higher current flow is measured in the vicinity of the GB rather than at the grain surfaces for CZTS (shown in Fig. 3 (a)). This implies that the GBs are acting as channels for current to flow rather than acting as strong recombination sites. In Fig. 3, dots are placed at the regions of high current. One can notice that all these dots correspond to a thin region between the GB core and the grain core. It appears that current is mainly flowing through the space adjacent to the GBs rather than the GB's core.

C-AFM measurements were performed on Cu-deficient CZTS thin film. In the measurements, the Pt tip is grounded and a negative bias (-0.5 V) is applied to the CZTS film. The spatial maps of topography in which the grains and GBs are clearly seen are shown in Fig. 3(a). Figure 3(b) shows the current mapping of CZTS thin film. Brighter contrast was observed at grains, which indicated higher currents at grains (20 nA) rather than at the grain boundaries**.**

3.4 Scanning Kelvin Probe Microscopy (SKPM) Studies

SKPM is a non-contact atomic force microscopy (AFM) mode that uses a conducting probe as a Kelvin probe to measure surface potential. The application of a direct current (*dc*) and alternating current (*ac*) voltage in general lead to an oscillating force experienced by the tip. This oscillating force has a *dc* component, an *ac* component with frequency of ω, and an *ac* component with frequency of 2ω. When the tip and the sample surface are at the same *dc* potential, the tip does not feel the *ac* oscillating force. Through the use of a feedback loop, it adjusts the *dc* potential to nullify this force component. A two-dimensional surface potential map can be derived from the *dc* potential[28].

The spatial maps of topography and the surface potential of CZTS have been investigated and the results are shown in Fig. 4 (a). The grains and GB can be identified by comparing the image contrast of the topography. The Cu-deficient CZTS thin film on Mo coated SLG demonstrate higher positive surface potential around GBs rather than the grain interior as shown in Fig. 4(b).

The average GB potential of CZTS in scanned region was measured to be ~ 75 mV. In the literature, GB potential for CZTS has been reported[26] to be

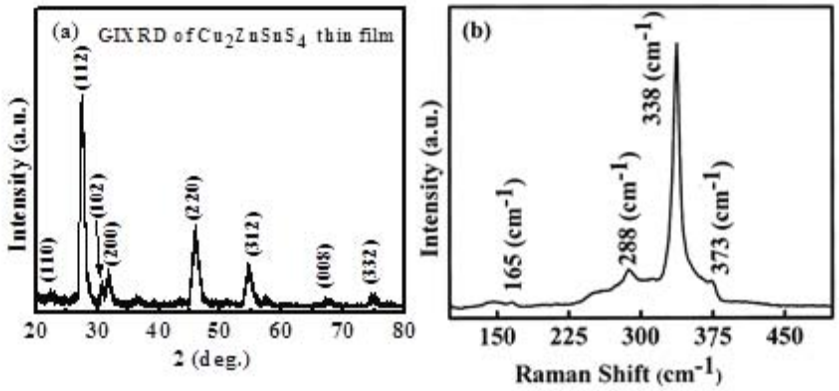

Fig. 2 — (a) XRD pattern of CZTS thin film and (b) Raman spectra of CZTS at room temperature

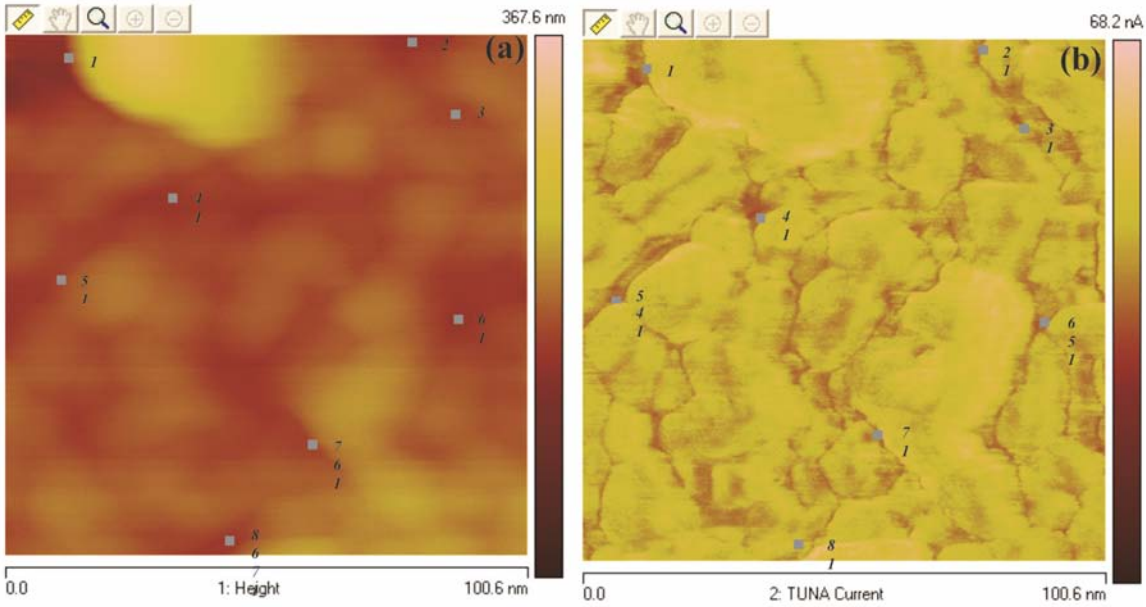

Fig. 3 — (a) Two-dimensional spatial maps of CZTS and (b) two-dimensional current spatial maps of CZTS at a sample bias of 0 V

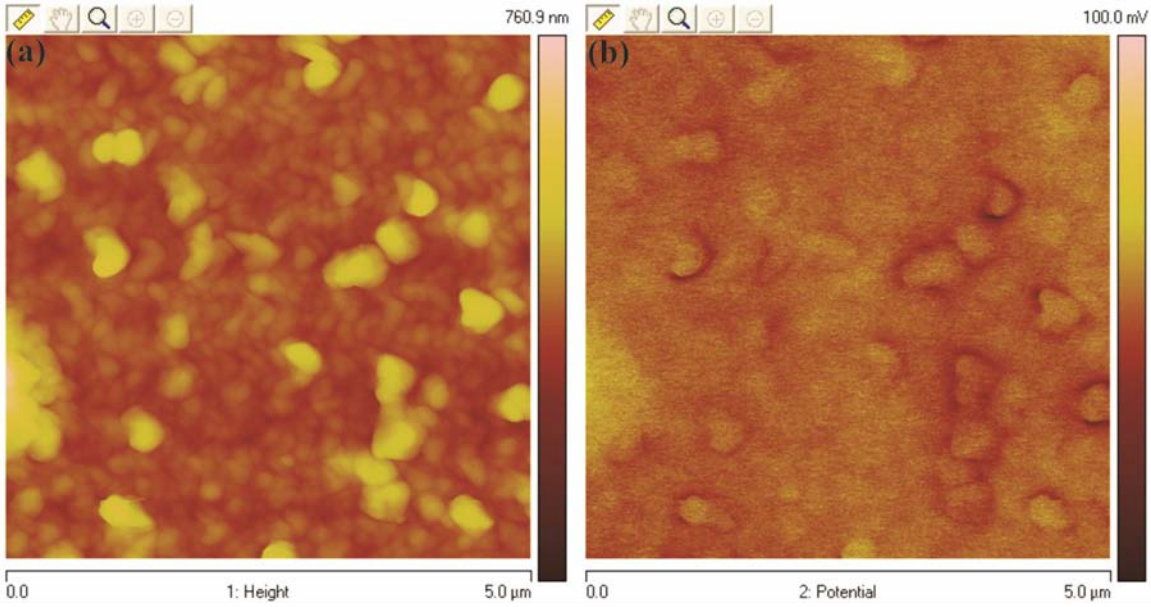

Fig. 4 — (a) Two-dimensional topographical spatial maps of CZTS and (b) two-dimensional surface potential spatial maps of CZTS

~ 200 mV. Our measurements indicated that grain interior (*p*-type) to GBs (*n*-type) has a smaller effective band gap than the bulk CZTS film. Since GBs in CIGS based thin film solar cells are responsible for higher efficiency, it further ascertained that CZTS film having similar GB properties[26] as CIGS solar cells have the potential to achieve similar high efficiency.

In the present study, an experimental demonstration of current flow at the adjacent regions of the GB core rather than the GBs in a solar cell material CZTS is shown. An explanation for this phenomenon is that the GB core has lower electron mobility as compared to the surrounding regions. Thus, electrons would preferentially flow in the region adjacent to the GB where the conductivity is higher. This phenomenon

has been demonstrated by Metzger in a simulation of CIGS solar cells where the GB has lower electron mobility as compared to the grain[27].

4 Conclusions

SKPM measurements carried out on CZTS thin film revealed a higher positive surface potential at the GBs compared to the grain while C-AFM measurements showed higher current flow in the vicinity of the GBs. These two measurement results are similar to those obtained for CIGS and CdTe and together they demonstrate that enhanced minority carrier collection is taking place at the GBs of CZTS. Since, CZTS solar cell has similar beneficial GB electronic properties as CIGS and CdTe, we theorize that CZTS solar cell has the potential to achieve the high efficiencies that CIGS and CdTe solar cells enjoy. This work has shown that the goal of achieving a low-cost, high efficiency solar cell composed of earth-abundant, non-toxic elements could be made possible through CZTS thin film solar cell.

Acknowledgement

Authors are thankful to Mr. J. Tawale for SEM/EDS, Dr. V. Toutam for AFM studies, CSIR-India and MNRE (Sanction No. 31/29/2010-11/PVSE) for the financial support. The authors are grateful to CSIR-India for TAP-SUN program. OPS and NM are thankful to University Grants Commission for Senior Research Fellowship.

References

1 Dhere N G, *Sol Energy Mater Sol Cells,* 91 (2007) 1376.
2 Singh OP, Muhunthan N, Singh V N, Samanta K & Dilawar N, *Mater Chem Phys,* 146 (2014) 452.
3 Singh OP, Muhunthan N, Singh V N & Singh B P, *Adv Mater Lett,* In-press (2014).
4 Muhunthan N, Singh O P, Thakur M K, Karthikeyan P, Singh D, Saravanan M, V N Singh, *J Sol Energ,* 2014 (2014) 476123.
5 Singh O P, Nadarajah M, Singh B P, Singh V N, *Adv Sci Engi Medic,* 6 (2014) 1.
6 Singh O P, Vijayan N, Sood K N, Singh B P, Singh V N, *J Alloys Compd,* 648 (2015) 595.
7 Jimbo K, Kimura R, Kamimura T, Yamada S, Maw W S, Araki H, Oishi K & Katagiri H, *Thin Solid Films,* 515 (2007) 5997.
8 Kumar Y B K, Bhaskar P U, Babu G S & Raja V S, *Phys Status Solidi A,* 207 (2010) 149.
9 Chan C P, Lam H & Surya C, *Sol Energy Mater Sol Cells,* 94 (2010) 207.
10 Schubert B-A, Marsen B, Cinque S, Unold T, Klenk R, Schorr S & Schock H-W, *Prog Photovolt* 19 (2011) 96.
11 Moriya K, Tanaka K & Uchiki H, *Jap J Appl Phys,* 47 (2008) 602.
12 Arora L, Gupta P, Chhikara N, Singh OP, Muhunthan N, Singh VN, et al. *Appl. Nanosci.* 5 (2015) 153.
13 Katagiri H, Saitoh K, Washio T, Shinohara H, Kurumadani T & Miyajima S, *Sol Energy Mater Sol Cells,* 65 (2001) 141.
14 Wang W, Winkler M T, Gunawan O, Gokmen T, Todorov T K, Zhu Y & Mitzi D B, *Adv Energy Mater,* 4 (2014) 1301465.
15 Dhankhar M, Singh O P, Singh V N, Renew, *Sust Energ Rev,* 40 (2014) 214.
16 Muhunthan N, Singh O P, Toutam V, Singh VN, *Mater Res Bullet*, 70 (2015) 373.
17 Muhunthan N, Singh O P, Singh V N, Sood K N, Rashmi, *Adv Mater Lett* 6 (2015) 290.
18 Muhunthan N, Singh OP, Singh S & Singh V N, *Int J Photoenergy*, 2013 (2013) 752012.
19 Zhou Y L, Zhou W H, Du Y F, Li M & Wu S X, *Mater Lett,* 65 (2011) 1535.
20 Zoppil G, I Forbes, Miles R W, Dale P J, Scragg J J & Peter L M, *Prog Photovolt,* 17 (2009) 315.
21 Fernandes P A, Salomé P M P & Cunha A F D, *Thin Solid Films,* 517 (2009) 2519.
22 P Fernandes A, Salomé P M P & Cunha A F D, *J Alloys Comp,* 509 (2011) 7600.
23 Azulay D, Millo O, Balberg I, Schock H-W, Visoly-Fisher I & Cahen D, *Sol Energy Mater Sol Cells,* 91 (2007) 85.
24 Shin R H, Jo W, Kim D W, Yun J H & Ahn S, *Appl Phys A,* 104 (2011) 1189.
25 Visoly-Fisher I, Cohen S R, Ruzin A & Cahen D, *Adv Mater,* 16 (2004) 879.
26 Li J B, Chawla V & Clemens B M, *Adv Mater,* 24 (2012) 720.
27 Metzger W K & Gloeckler M, *J Appl Phys,* 98 (2005) 063701.
28 Schroder D K, Semiconductor material and device characterization, Wiley-IEEE Press, Hoboken, N J, USA (2006).